XLVI CILAMCE
VITÓRIA - ES - BRAZIL - 2025
XLVI IBERO-LATIN AMERICAN CONGRESS ON COMPUTATIONAL METHODS IN ENGENEERING

Modeling the Structural Response of Steel Frames Equipped with Tuned Liquid Damper under Seismic Excitation in OpenSees

Juan F. V. Ospina[1], Letícia F. F. Miguel[2], Jesús D. Villalba-Morales[3]

[1]*Postgraduate Program in Civil Engineering (PPGEC), Federal University of Rio Grande do Sul (UFRGS)*
Av. Osvaldo Aranha, 99, 90035-190, Porto Alegre-Rio Grande do Sul, Brazil
juan.vallejo@ufrgs.br
[2]*Department of Mechanical Engineering (DEMEC), Postgraduate Program in Mechanical Engineering (PROMEC), Postgraduate Program in Civil Engineering (PPGEC) Federal University of Rio Grande do Sul (UFRGS)*
Av. Sarmento Leite, 425, 90050-170, Porto Alegre-Rio Grande do Sul, Brazil
letffm@ufrgs.br
[3]*Department of Civil Engineering, School of Engineering, Pontifical Xavierian University,*
Cra 7 No 40 - 62, 110231, Bogotá, Colombia
jesus.villalba@javeriana.edu.co

Abstract. Tuned Liquid Dampers (TLDs) are passive devices for structural vibration control that stand out for their low cost and efficiency, making them attractive for civil engineering applications, especially in slender or high-rise buildings subjected to dynamic loads such as wind or earthquakes. These systems operate by tuning the fundamental sloshing frequency of the contained liquid to match the natural frequency of the structure's dominant mode, generating inertial forces that counteract structural motion. This study numerically investigates the performance of a rooftop-mounted TLD on a steel Moment-Resisting Frame (MRF) using OpenSees, considering both harmonic resonant excitations and representative earthquake ground motions. The TLD is modeled using an Equivalent Mechanical Model (EMM) based on Housner's analogy, which simulates the liquid's behavior through a coupled mass-spring-damper system. The results demonstrate that the EMM provides accurate predictions under low excitation amplitudes and high structural damping, effectively reducing structural response. Nonetheless, the damper's efficiency diminishes progressively with increasing liquid depth-to-length ratio (h/L), revealing a trade-off that highlights the critical role of geometric tuning in maximizing TLD performance.

Keywords: Tuned Liquid Damper (TLD), Seismic exitations, Vibration Control, Equivalent Mechanical Model (EMM)

1 Introduction

Structures with vertical irregularities, specifically as setbacks, tend to exhibit complex dynamic behavior during seismic events due to stress redistribution and amplified drift demands at stiffness discontinuities [1]. These effects often compromise structural performance, particularly in seismic zones. To mitigate these adverse effects, upplemental damping systems are typically required to complement conventional design strategies. Among passive control solutions—valued for their cost-effectiveness, ease of installation, and minimal maintenance—several mechanisms have been developed, including metallic dampers [2, 3], friction dampers [4, 5], viscous dampers [6, 7], and viscoelastic dampers[8, 9].Additionally, inertia-based systems like Tuned Mass Dampers (TMDs) [10, 11] and Tuned Liquid Dampers (TLDs) ignificant interest for their dynamic performance. In particular, TLDs offer a practical and versatile alternative, dissipating energy through the sloshing motion of a liquid column. These systems are particularly advantageous as they eliminate the need for auxiliary solid masses or supplemental damping and stiffness elements [12].

Originally proposed by Froude [13] formitigating ship rolling motion, TLDs dissipate energy through the oscillatory sloshing of fluid within partially filled containers. Their natural sloshing frequency is tuned to the structure's dominant vibrational mode. The integration into seismic engineering was pioneered by Fujino et al. [14], who demonstrated their effectiveness in reducing structural resonances through fluid–structure interaction. Since then, numerous studies have validated their seismic performance across a wide range of structural systems (e.g., Konar and Ghosh [15, 16]).

Traditional fluid models have been superseded by advanced fluid-structure interaction approaches that better represent the actual tank behavior. Although these approaches offer high-fidelity simulations of nonlinear phenomena such as wave breaking and turbulence, their practical application in structural engineering is limited by modeling complexity and high computational cost. To balance accuracy with computational efficiency, researchers have developed equivalent mechanical models that simulate sloshing dynamics through coupled mass-spring-damper analogies (e.g.,Tait [17], Das et al. [18], Konar et al. [19]). Accordingly, the present study adopts the rheological model developed by Housner, which captures the essential effects of fluid-structure coupling with low computational demand. This simplified formulation facilitates implementation in dynamic simulation platforms such as OpenSees and enables efficient analysis of the seismic performance of frames with vertical irregularities equipped with TLDs.

2 Equivalent mechanical model of the structure-TLD

A structure incorporating a vibration control system—such as a TLD can be idealized as a single-degree-of-freedom (SDOF) shear building model, as shown in Figure 1a). The seismic response of this TLD-equipped structure is governed by the following system of equations:

$$\mathbf{M}\ddot{x}(t) + \mathbf{C}\dot{x}(t) + \mathbf{K}x(t) = -\mathbf{M}l\ddot{x}_g(t) + \mathbf{Z}(t) \tag{1}$$

In this formulation, M, C, and K denote the mass, damping, and stiffness matrices of the SDOF system, respectively. The vector $x(t)$ represents the relative displacement of each floor at time t, while $\dot{x}$ and $\ddot{x}$ indicating the corresponding velocity and acceleration, l is the influence vector, and $\ddot{x}_g(t)$ denotes the ground acceleration due to seismic input. The term $Z(t)$ accounts for the force contribution from the damping device.

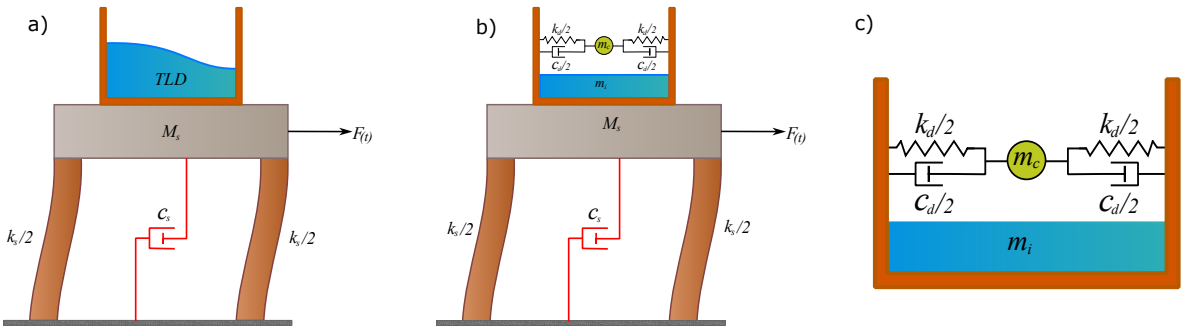


Figure 1. Schematic diagram of SDOF mathematical model (a) equipped with TLD (b) Structure with an equivalent mechanical model of TLD and c) Mechanical model for the TLD system.

The liquid motion in a TLD can be represented using an equivalent spring-mass-dashpot system [20], where the mechanical analog captures the fundamental sloshing dynamics while maintaining computational efficiency. In this framework, Housner [21] decomposes the liquid's dynamic response into two distinct components observable in Fig. 1b–c: (1) impulsive pressures generated by the container's rigid acceleration, and (2) convective pressures arising from surface wave oscillations, thus modeling the complete fluid-structure interaction system. A TLD can thus be represented using the analogy of a TMD, where the sloshing dynamics are characterized by an equivalent convective mass m_c, stiffness k_d, damping coefficient c_d, and natural frequency ω_d. These parameters govern the energy dissipation and tuning behavior of the system, and their estimation can be found in several works available in the literature [15, 18].

$$\omega_d = \sqrt{\frac{\pi g}{L}\tanh\frac{\pi d}{L}} \tag{2}$$

$$m_c = M_0\frac{8L}{d\pi^3}\tanh\frac{\pi d}{L} \tag{3}$$

$$k_d = m_s\frac{\pi g}{L}\tanh\frac{\pi d}{L} \tag{4}$$

$$c_d = \sqrt{2}\frac{m_c}{\eta + d}\sqrt{\omega_d\lambda}\left[1 + \frac{2d}{B} + S\right] \tag{5}$$

Here, B, d, and L denote the internal width, liquid depth, and internal length of the TLD, respectively. The gravitational acceleration, the kinematic viscosity of water, and the total liquid mass are represented by g, ν, and M_0, respectively. η is the maximum amplitude of liquid sloshing, since the sloshing is untuned, η remains small and the approximation $(\eta + d) \approx d$ is valid. In the present case, S is the surface contamination factor, whose value may be taken as unity according to Miles [22].

3 Numerical example

3.1 Details of example buildings

This investigation examined three nine-story steel moment-resisting frames (MRFs), comprising: (i) a geometrically regular reference structure, and (ii) two vertically irregular configurations featuring distinct geometric setbacks. The regular frame serves as a baseline model, adopting the well-established configuration proposed by Karavasilis et al. [23], characterized by uniform story heights of 3.0 m and consistent bay widths of 5.0 m throughout its elevation (Fig. 2a). All structural members—including beams, columns, and connections—were modeled using conventional hot-rolled steel sections with a modulus of elasticity $E = 200$ GPa and mass density $\rho = 7850$ kg/m^3. Complete section properties and member sizes are systematically cataloged in Table 1.

Table 1. Column and beam sections of the studied building [23]

Story	1	2–5	6–7	8–9
Column	HEB 360	HEB 360	HEB 340	HEB 320
Beam	IPE 360	IPE 400	IPE 360	IPE 330

The irregular frame variants were strategically derived from this reference configuration by introducing two contrasting setback patterns: The first irregular configuration (Fig. 2b) incorporates significant upper-story setbacks, producing a tapered profile that modifies both stiffness and mass distribution in the upper third of the structure. The second irregular configuration (Fig. 2c) adopts a more pronounced tower-like morphology with a substantial lower-story setback, following the seismic-resistant architectural scheme investigated by Karavasilis et al. [24].

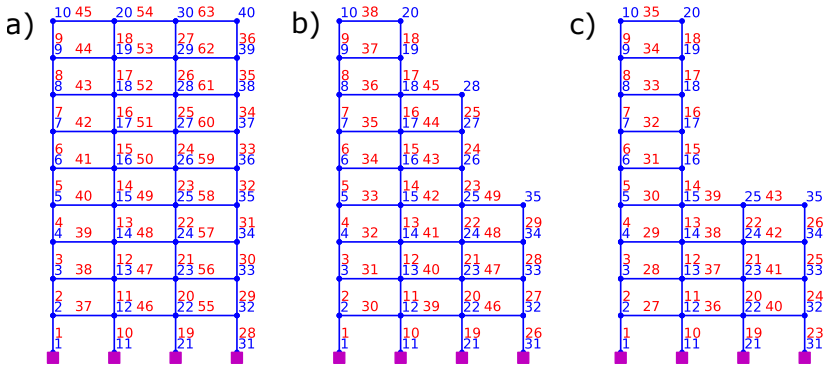


Figure 2. Steel MRF configurations: (a) IR0, (b) IR1, (c) IR3. [24]

A two-dimensional linear elastic finite element model was implemented in OpenSees to simulate the seismic response of the steel moment-resisting frames. The structural system was discretized using nodes with three degrees of freedom (two translational and one rotational) to capture planar behavior, with beam-column elements modeled using the *elasticBeamColumn* formulation incorporating corotational geometric transformation. Column base supports were fully constrained to represent fixed foundation conditions. Seismic excitation was applied as uniform base motion in the horizontal direction through the *UniformExcitation* command. System damping was modeled using a Rayleigh formulation with 0.5% critical damping ratio calibrated to the first two vibrational modes, consistent with values for bare steel structures. The tuned liquid dampers were simulated through a parallel combination of elastic spring and viscous damper elements defined using the *uniaxialMaterial* command, with

force transfer to the structural system achieved through *rigidLink* elements of beam type connected to the top story.

3.2 Harmonic Excitation

The first excitation considered is a harmonic ground motion, modeled as a sinusoidal signal with a frequency equal to the fundamental period of each structure. This allows reproduction of resonance conditions and evaluation of the structural response under controlled dynamic amplification. It serves as a benchmark to assess the efficiency of the Tuned Liquid Damper (TLD) in dissipating energy when the excitation frequency matches the system's natural frequency. The harmonic motion is defined by a amplitude A = 5cm and a duration of 10 seconds. The fundamental frequencies of the three analyzed structures—one regular and two with vertical setbacks—are presented in Table 2, obtained from modal analysis of the bare frames (without TLD).

Table 2. Fundamental periods and modal mass participation

Structure	Frequencies (Hz)	Mass Participation (%)
IR0	3.04, 8.70, 15.91	79.60, 10.39, 3.83
IR1	3.63, 8.73, 15.38	74.42, 13.21, 3.93
IR2	3.59, 7.80, 15.56	60.78, 25.78, 3.64

3.3 Artificial Seismic Excitation

The second type of excitation consists of an artificially generated seismic signal based on the Kanai–Tajimi power spectral density (PSD) model [25], which captures the frequency-dependent amplification effects of local soil conditions, as defined in eq. (6). The Kanai–Tajimi filter parameters used in this study include a damping ratio of 0.6 and a predominant soil frequency of 5π rad/s. To obtain a non-stationary acceleration time history in the time domain, the target PSD is transformed using the stochastic simulation method proposed by Shinozuka and Jan [26], following the formulation in eq. (7). The artificial ground motion is generated over a frequency range of 0 to 25Hz, with a normalized peak ground acceleration of 0.625g and a total signal duration of 20 seconds, assuming rigid soil conditions. The final signal is illustrated in Fig. 3.

$$S(w) = S_0 \left[\frac{w_s^4 + 4w_s\xi_s^2 w}{(w^2 - w_s^2) + 4w_s^2\xi_s^2 w^2} \right], \qquad S_0 = \frac{0.03\xi_s}{\pi w_s(4\xi_s^2 + 1)}. \tag{6}$$

$$\ddot{y}(t) = \sqrt{2}\sum_{j=1}^{N_w} \sqrt{S(w_j)\Delta w}\cos(wt + \phi_j) \tag{7}$$

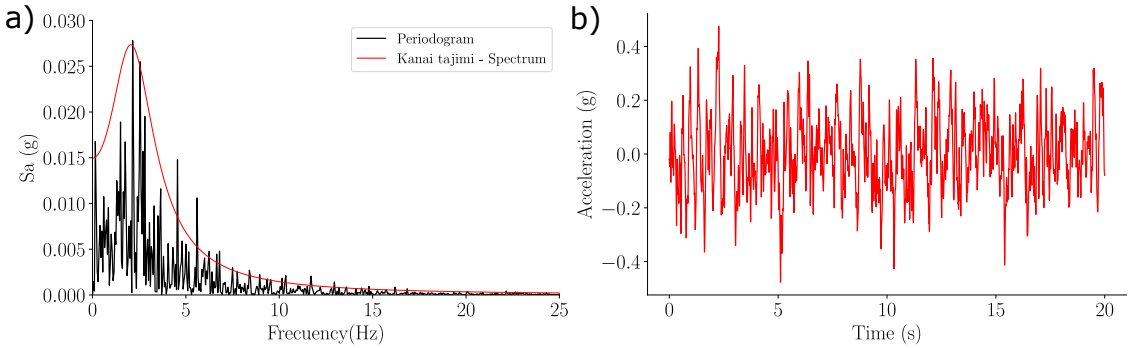


Figure 3. (a) Power spectral density (PSD) of the Kanai-Tajimi model; (b) artificial accelerogram generated via the Shinozuka-Jan method.

4 Results and discussions

The TLDs implemented in this study were designed with a tuning ratio of 1.0%, a mass ratio of 5%, and a depth ratio of 50%, and were installed at the top story of each structure to maximize their vibration control efficiency. To evaluate their performance, the first stage of analysis involved harmonic excitation at the fundamental frequency of each frame. The results, shown in Figure 4 to 6, demonstrate a clear reduction in top floor accelerations due to the presence of TLDs, highlighting their effectiveness in mitigating resonant amplification. In the second stage, nonlinear time-history analyses were conducted to assess interstory drift demands. As illustrated in Figures 7 to 9, the inclusion of TLDs led to a notable decrease in drift across the height of the structures. A summary of the numerical results for both peak acceleration and maximum interstory drift is presented in Table 3, which consolidates the response metrics across all structural configurations.

Table 3. Relative reduction of maximum story drift using Tuned Liquid Dampers (TLD)

Structure	Max Top Floor Acceleration		Relative	Max Story Drift (%)		Relative
	w/o TLD (%)	with TLD (%)	reduction (%)	w/o TLD (%)	with TLD (%)	reduction (%)
IR0	111.6669614	24.4806122	78.08	0.92	0.85	6.95
IR1	124.9410127	20.8947707	83.28	1.02	0.37	64.01
IR2	135.1837202	19.5792384	85.52	0.99	0.62	37.11

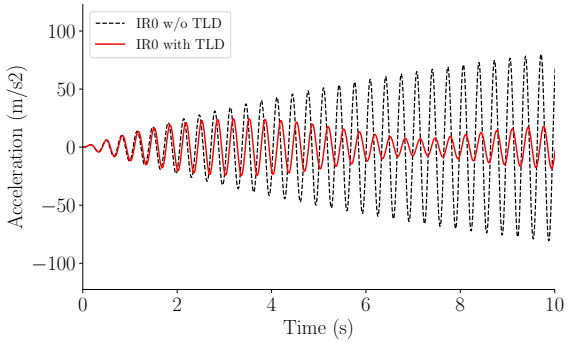


Figure 4. Top Floor Acceleration under Harmonic Excitation IR0: With vs. Without TLD

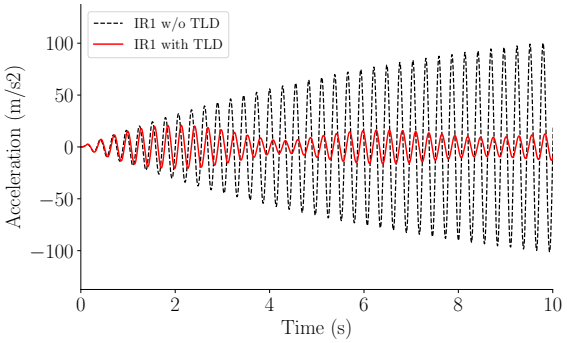


Figure 5. Top Floor Acceleration under Harmonic Excitation IR1: With vs. Without TLD

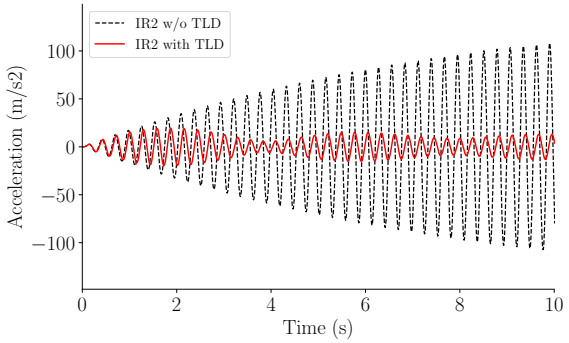


Figure 6. Top Floor Acceleration under Harmonic Excitation IR2: With vs. Without TLD

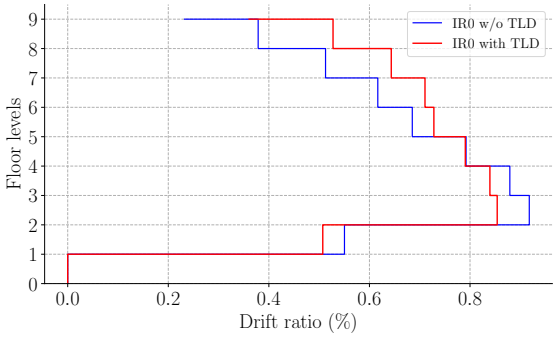


Figure 7. Story Drift IR0 with and without TLD

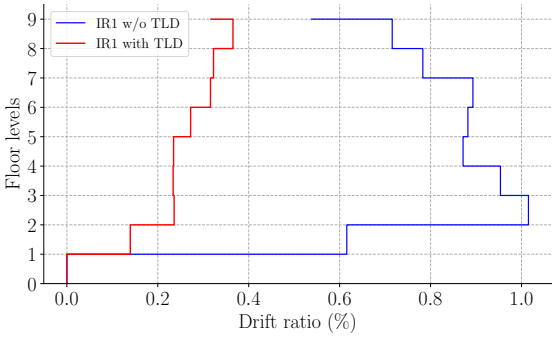


Figure 8. Story Drift IR1 with and without TLD

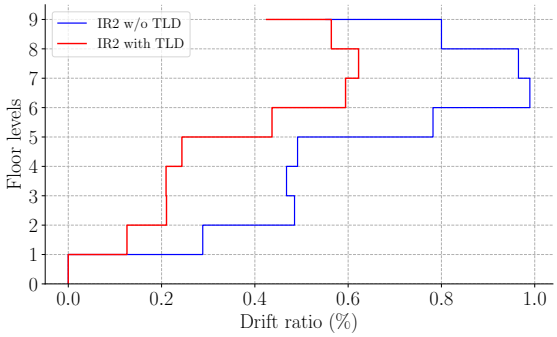


Figure 9. Story Drift IR2 with and without TLD

5 Conclusions

This study substantiates the significant efficacy of Tuned Liquid Dampers (TLDs) in mitigating seismic responses of steel moment-resisting frames (MRFs). Results demonstrate pronounced reductions in resonant peak accelerations and interstory drift ratios (IDRs), particularly for irregular configurations. The attenuation of dynamic amplification near structural resonance underscores TLDs' capacity to enhance overall seismic performance by suppressing critical vibration modes.

While the classical Housner model provided a computationally efficient framework for TLD simulation, its utility resides primarily in preliminary design stages. This lumped-mass analogy offers pragmatic initial sizing estimates but does not supersede high-fidelity numerical models (e.g., CFD-FEM coupled approaches) for capturing nonlinear sloshing, wave breaking, and complex fluid-structure interaction (FSI) phenomena. Such advanced methodologies remain indispensable for performance-critical designs and validating TLD effectiveness under multi-hazard scenarios.

Importantly, the application of optimization techniques to tune TLD parameters—such as tuning ratio, mass ratio, and damping characteristics—holds great promise for maximizing the benefits of these devices. Tailoring the damper design through systematic optimization can significantly enhance vibration control efficiency, enabling the TLD to be a viable and effective option in seismic mitigation strategies. Future research should continue exploring advanced modeling approaches and optimization frameworks to fully exploit the capabilities of TLD systems in seismic control.

Acknowledgements. The authors acknowledge the financial support of Conselho Nacional de Desenvolvimento Científico e Tecnológico (CNPq) and Coordenação de Aperfeiçoamento de Pessoal de Nível Superior (CAPES), Brazil.

Authorship statement. The authors hereby confirm that they are the sole liable persons responsible for the authorship of this work, and that all material that has been herein included as part of the present paper is either the property (and authorship) of the authors, or has the permission of the owners to be included here.

References

[1] H. Shakib and M. Pirizadeh. Probabilistic seismic performance assessment of setback buildings under bidirectional excitation. *Journal of Structural Engineering*, vol. 140, n. 2, pp. 04013061, 2014.
[2] R. Aghlara and M. M. Tahir. A passive metallic damper with replaceable steel bar components for earthquake protection of structures. *Engineering structures*, vol. 159, pp. 185–197, 2018.
[3] D. Henao-Leon, L. F. F. Miguel, and J. D. Villalba-Morales. A proposal for the optimization of the geometric configuration of a hollow cylindrical steel damper with slots. *Journal of the Brazilian Society of Mechanical Sciences and Engineering*, vol. 45, n. 3, pp. 152, 2023.
[4] L. F. F. Miguel, L. F. F. Miguel, and R. H. Lopez. Robust design optimization of friction dampers for structural response control. *Structural Control and Health Monitoring*, vol. 21, n. 9, pp. 1240–1251, 2014.
[5] S. P. Ontiveros-Pérez, L. F. F. Miguel, and J. D. Riera. Reliability-based optimum design of passive friction dampers in buildings in seismic regions. *Engineering Structures*, vol. 190, pp. 276–284, 2019.
[6] G. M. Del Gobbo, M. S. Williams, and A. Blakeborough. Comparing fluid viscous damper placement methods considering total-building seismic performance. *Earthquake Engineering & Structural Dynamics*, vol. 47, n. 14, pp. 2864–2886, 2018.
[7] J. Zhong, Z. Hu, W. Yuan, and L. Chen. System-based probabilistic optimization of fluid viscous dampers equipped in cable-stayed bridges. *Advances in Structural Engineering*, vol. 21, n. 12, pp. 1815–1825, 2018.
[8] Z.-D. Xu. Earthquake mitigation study on viscoelastic dampers for reinforced concrete structures. *Journal of Vibration and Control*, vol. 13, n. 1, pp. 29–43, 2007.
[9] Z.-D. Xu, T. Ge, and J. Liu. Experimental and theoretical study of high-energy dissipation-viscoelastic dampers based on acrylate-rubber matrix. *Journal of Engineering Mechanics*, vol. 146, n. 6, pp. 04020057, 2020.
[10] L. F. Fadel Miguel, R. H. Lopez, L. F. F. Miguel, and A. J. Torii. A novel approach to the optimum design of mtmds under seismic excitations. *Structural Control and Health Monitoring*, vol. 23, n. 11, pp. 1290–1313, 2016.
[11] A. M. Ramírez Ospina, J. A. González Muñoz, O. Cundumi Sánchez, and J. D. Villalba Morales. Optimización del diseño de estructuras conformadas por pórticos de acero resistentes a momentos y amortiguadores de masa sintonizada (tmd). *Ciencia e Ingeniería Neogranadina*, vol. 31, n. 2, pp. 9–25, 2021.
[12] T. Konar and A. Ghosh. A review on various configurations of the passive tuned liquid damper. *Journal of Vibration and Control*, vol. 29, n. 9-10, pp. 1945–1980, 2023a.
[13] W. Froude. On the rolling of ships. *Transaction of the Institution of Naval Architects*, vol. 2, 1861.
[14] Y. Fujino, L. Sun, B. M. Pacheco, and P. Chaiseri. Tuned liquid damper (tld) for suppressing horizontal motion of structures. *Journal of engineering mechanics*, vol. 118, n. 10, pp. 2017–2030, 1992.
[15] T. Konar and A. D. Ghosh. Flow damping devices in tuned liquid damper for structural vibration control: a review. *Archives of Computational Methods in Engineering*, vol. 28, n. 4, pp. 2195–2207, 2021.
[16] T. Konar and A. D. Ghosh. Adaptive design of an overhead water tank as dynamic vibration absorber for buildings by use of a stiffness-varying support arrangement. *Journal of Vibration Engineering & Technologies*, vol. 11, n. 3, pp. 827–843, 2023b.
[17] M. Tait. Modelling and preliminary design of a structure-tld system. *Engineering Structures*, vol. 30, n. 10, pp. 2644–2655, 2008.
[18] A. Das, T. Konar, D. Maity, and S. K. Bhattacharyya. Revisiting equivalent tuned mass damper analogy for tuned liquid damper utilizing cfd-fea framework. *Soil Dynamics and Earthquake Engineering*, vol. 172, pp. 108051, 2023.
[19] T. Konar, A. Das, and A. D. Ghosh. Near-fault earthquake-induced vibration control of a supertall benchmark building using an inerter-assisted compliant liquid damper. *ASCE-ASME Journal of Risk and Uncertainty in Engineering Systems, Part A: Civil Engineering*, vol. 10, n. 4, pp. 04024070, 2024.
[20] F. T. Dodge and others. The new" dynamic behavior of liquids in moving containers", 2000.
[21] G. W. Housner. The dynamic behavior of water tanks. *Bulletin of the seismological society of America*, vol. 53, n. 2, pp. 381–387, 1963.
[22] J. W. Miles. Surface-wave damping in closed basins. *Proceedings of the Royal Society of London. Series A. Mathematical and Physical Sciences*, vol. 297, n. 1451, pp. 459–475, 1967.
[23] T. L. Karavasilis, N. Bazeos, and D. E. Beskos. Drift and ductility estimates in regular steel mrf subjected to ordinary ground motions: a design-oriented approach. *Earthquake Spectra*, vol. 24, n. 2, pp. 431–451, 2008a.
[24] T. L. Karavasilis, N. Bazeos, and D. Beskos. Seismic response of plane steel mrf with setbacks: Estimation of inelastic deformation demands. *Journal of Constructional Steel Research*, vol. 64, n. 6, pp. 644–654, 2008b.
[25] K. Kanai. An empirical formula for the spectrum of strong earthquake motion. In *Proceedings of the Second World Conference on Earthquake Engineering*, 1961.
[26] M. Shinozuka and C.-M. Jan. Digital simulation of random processes and its applications. *Journal of sound and vibration*, vol. 25, n. 1, pp. 111–128, 1972.